

Language Modeling at Scale

Mostofa Patwary, Milind Chabbi, Heewoo Jun,
Jiaji Huang, Gregory Diamos, and Kenneth Church
Silicon Valley AI Lab, Baidu Research
Sunnyvale, California, USA

Corresponding Author: patwarymostofa@baidu.com

Abstract—We show how Zipf’s Law can be used to scale up language modeling (LM) to take advantage of more training data and more GPUs. LM plays a key role in many important natural language applications such as speech recognition and machine translation. Scaling up LM is important since it is widely accepted by the community that there is no data like more data. Eventually, we would like to train on terabytes (TBs) of text (trillions of words). Modern training methods are far from this goal, because of various bottlenecks, especially memory (within GPUs) and communication (across GPUs). This paper shows how Zipf’s Law can address these bottlenecks by grouping parameters for common words and character sequences, because $U \ll N$, where U is the number of unique words (types) and N is the size of the training set (tokens). For a local batch size K with G GPUs and a D -dimension embedding matrix, we reduce the original per-GPU memory and communication asymptotic complexity from $\Theta(GKD)$ to $\Theta(GK + UD)$. Empirically, we find $U \propto (GK)^{0.64}$ on four publicly available large datasets. When we scale up the number of GPUs to 64, a factor of 8, training time speeds up by factors up to $6.7\times$ (for character LMs) and $6.3\times$ (for word LMs) with negligible loss of accuracy. Our weak scaling on 192 GPUs on the Tieba dataset shows a 35% improvement in LM prediction accuracy by training on 93 GB of data ($2.5\times$ larger than publicly available SOTA dataset), but taking only $1.25\times$ increase in training time, compared to 3 GB of the same dataset running on 6 GPUs.

I. INTRODUCTION

This paper will show how Zipf’s Law [1]–[3] can be used to help scale up language modeling (LM) to take advantage of more training data and more GPUs. Zipf’s law is known to hold across many languages and wide variety of data sets [4], [5]. Zipf’s law makes it clear that there are many more tokens than types, as illustrated in Figure 1. It is common in language modeling to distinguish types (unique words) from tokens (non-unique words). For example, the phrase, “to be or not to be,” consists of four types and six tokens.

In general, the number of *unique* words in a training step is significantly smaller than the total number of tokens (the per-GPU batch size times the number of GPUs) and grows as a power law. Figure 1 shows the number of types (unique words, U) on the y-axis as a function of tokens (non-unique words, N) along the x-axis. The figure shows four datasets: 1-Billion word [6] (1b), Gutenberg [7] (gb), Common crawl [8] (cc), and Amazon review [9] (ar). All four lines fall well below the red line ($x = y$), labeled *batch*. This gap indicates an important opportunity for improvement. The data fit a power law: $U \propto N^{0.64}$. When N is 40-million total tokens in a training step,

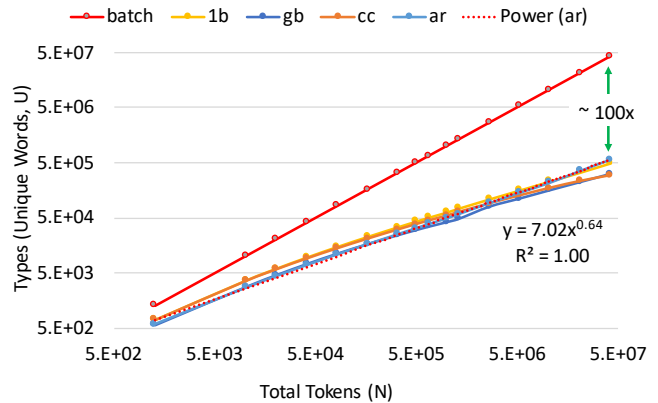


Fig. 1. There are many more words (tokens) than unique words (types). The red line is a baseline for $x = y$. The gap between the data and the red line is large (even on *log*-scales), and increases as we scale up batch sizes and GPUs. The 4 lines correspond to 4 datasets: one Billion word (1b), Gutenberg (gb), Common Crawl (cc), and Amazon Review (ar).

TABLE I
DATASETS

Datasets	# Characters	# Words	Bytes	Language
1-Billion Word [6] (1b)	4.19B	0.78B	3.94GB	English
Gutenberg [7] (gb)	8.90B	1.81B	8.29GB	English
Amazon Review [9] (ar)	38.76B	7.01B	37.04GB	English
Tieba [10]	34.36B	NA	93.12GB	Chinese

the number of unique words, U , is $\sim 100\times$ smaller; and the gap continues to grow with N .

Language modeling is a fundamental task in natural language processing (NLP) and language understanding. It predicts the next token (e.g. words, sub-words, or characters) given the context (a sequence of surrounding tokens). Language modeling plays an important role in so-called noisy channel applications such as speech recognition, OCR and spelling correction [11]. The noisy channel was introduced by Shannon [12], [13], and continues to be used in a number of more recent applications such as: natural language generation [14], machine translation [15], speech recognition [16], and text summarization [17], to name a few. In the rest of this paper we use the abbreviation LM to mean Language Modeling or Language Model, which will be obvious from the context.

There is no data like more data. More data (and larger models) produce better estimates of sentence probabilities. Recent techniques leverage such large corpora by pre-training a neural language model and using the learned hidden representations

to fine-tune on various NLP tasks. This simple but highly effective approach has achieved state-of-the-art results across many natural language understanding tasks that have benefited from domain expertise and specialized architectures [18], [19].

Unfortunately, more data and larger models also increase the training time [20], [21]. It is therefore of significant interest to accelerate the training time of language modeling, specially by scaling the models to take advantage of the compute capability of high performance computing (HPC) resources such as GPUs. Although there have been several recent efforts to scale deep learning models in computer vision applications [22]–[24], less has been written on scaling language models and natural language processing applications. There are a couple of recent papers that scale LM implementations to a small number of GPUs [25], [26]. If we are going to scale up to terabytes, we will need to find a way to scale up to take advantage of many more GPUs. This work presents an important step in that direction.

Scaling is challenging because the vocabulary (number of types) is large, and the training corpus (number of tokens) is even larger. Modern neural network based methods make use of word or character embeddings that tend to be large enough to run into memory and communication bottlenecks. Unlike vision-related application, which employ an ALLREDUCE over the gradients on all GPUs to update the local parameters on each GPU, LM-based applications cannot employ ALLREDUCE due to the *word/char embeddings*. Instead, NLP applications use ALLGATHER operation over the embedding gradients, which results in memory demands and communication volume to grow proportional to the *product of the number of GPUs and the batch size per GPU*. We elaborate more on the challenges in Section II.

Prior work on scaling LMs tend to simplify the problem by limiting the size of the vocabulary, or limited the number of GPUs. For example, [25] limited the vocabulary to just $\sim 24K$ words, a small fraction of the words in the corpus, a large common crawl dataset [8]. Another example, [26], uses a large vocabulary, $\sim 260K$, but only four GPUs. The most recent study on large scale language modeling [21] demonstrates a scaling of up to 128 GPUs but considers only character language models, where the vocabulary is tiny (~ 100).

This work will introduce three optimizers for scaling up:

- 1) *Uniqueness*: There are many fewer types than tokens ($U \ll N$) because of Zipf’s law. This observation allows us to turn a large, expensive ALLGATHER operation, employed in the *input* word embedding layer, into a small ALLGATHER followed by an ALLREDUCE operation, which changes the asymptotic complexity of memory and communication needed for updating gradients.
- 2) *Seeding*: The so-called *sampled softmax* [27] employed in LMs to reduce the computational demands renders the *uniqueness* technique useless in LM’s *output* word embedding layer, because each GPU chooses a random subset of words, disobeying the word-frequency distribution. We enforce a controlled randomization that obeys the power-law of word frequency distribution, which

allows us to reap the benefits of *uniqueness* in the output word embedding layer.

- 3) *Compression*: Finally, we employ half-precision floating-point (FP16) numbers for data used in communication to further reduce bandwidth demands. FP16 reduces the communication volume by 50%. We recover the accuracy loss due to the lower precision via *compression-scaling*.

Uniqueness and *seeding* reduce the asymptotic bounds of both communication volume and GPU memory size. *Compression* reduces the communication volume by a constant factor. We evaluate our optimizations on four large datasets (three publicly available and one internal). Experimental evaluation demonstrates significant reduction in memory (within a GPU) and communication (across GPUs). Our technique shows $8.6\times$ memory reduction, which leads to $6.3X$ speedup for word LMs. We demonstrate $6.7\times$ (character LM) and $6.3\times$ (word LM) speedup by scaling to 64 GPUs ($8\times$ more) with negligible loss of accuracy. Finally, we demonstrate weak scaling on Baidu *Tieba*¹ Chinese corpus (internal). This paper will use a relatively small sample of what’s available. But even so, the sample of 93 GB we use is large enough to raise interesting scaling challenges: $2.5\times$ larger than the publicly available state-of-the-art dataset. Compared to a 3GB of the same dataset using 6 GPUs, when we scale to $32\times$ more GPUs and data (192 GPUs and 93 GB, respectively), the running time increases by only $1.25\times$, but provides an accuracy improvement of 35%.

The paper is organized as follows. Section II describes the LM scaling challenges; Section III describes our techniques for scaling LM. Section IV and V provide experimental setting and empirical results, respectively. Section VI discusses the related works, and Section VII concludes the paper.

II. BACKGROUND: CHALLENGES IN SCALING LM

In this section we overview the state-of-the-art workflow for RNN-based language modeling. Figure 2 represents an anecdotal RNN-based language model akin to Bengio et al. [28]. It consists of an input embedding, several feed-forward or recurrent (i.e. RNN) layers, an output embedding, followed by a softmax classifier layer.

A. Language Model Basics

LMs employ dictionary of commonly used terms. For example, all letters (alphabets, numbers, punctuation) in a language forms the vocabulary for a *character* LM, whereas all words in the dictionary form the vocabulary for a *word* LM. A “word” is a unique entry in the vocabulary and a “token” is an instantiation of a word in a training set.

Assume a vocabulary V of $|V|$ words. Given a sequence of K training tokens $w_1, w_2, w_3, \dots, w_K$, where each $w_i \in V$, one can naively produce a $K \times |V|$ activation matrix A as an input to RNN layers. In this matrix, if i^{th} input token is the j^{th} word in V , $A[i][j]$ will be set to 1. Such matrix will be extremely large for a large vocabulary, filled largely with

¹<https://tieba.baidu.com>

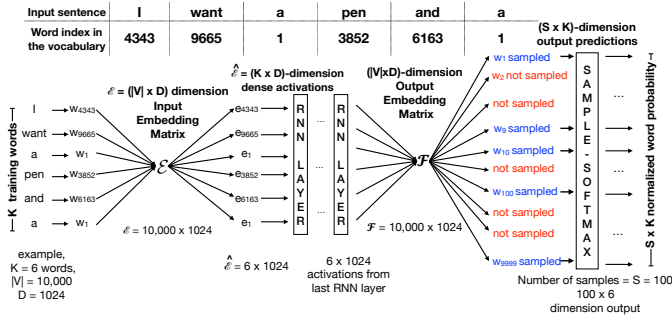


Fig. 2. A schematic diagram of a typical RNN-based LM for a vocabulary V and embedding dimension D . A $|V| \times D$ embedding matrix projects the input K token sequence into a dense $K \times D$ matrix as the activations for the first RNN layer. After passing through the various number of RNN layers, a $|V| \times D$ output embedding matrix projects the prediction of each word in the vocabulary. For reducing the computational complexity, only a small number $S \ll |V|$ of words of the vocabulary are sampled and their normalized probabilities are computed by the sampled softmax layer.

zeros, and computationally very expensive for the subsequent layers of the neural network.

LMs employ an “embedding layer” to reduce this size of activation input to the neural network. Different words with related sentiments produce similar *embedding vectors*, which are indistinguishable by the RNN layers. The *input* embedding layer projects the large, sparse input sequence of tokens into a small, dense matrix \hat{E} . To obtain \hat{E} , the model simply hash maps every input token w_i to a D -dimensional vector e_{w_i} of real numbers, where $D \ll |V|$, and produces a $K \times D$ dimension matrix. The mapping uses a $|V| \times D$ embedding matrix \mathcal{E} . The real numbers forming the embedding matrix \mathcal{E} are learned during the training process.

Figure 2 exemplifies this process. The input is a six-token sequence “I want a pen and a”, where the word-index of each token is shown at the top of the figure. The first token “I” is 4343th word in the vocabulary. The token “a” appears twice, once at position three and again at position six, which becomes important during the back-propagation. The first row of the dense, activation matrix \hat{E} will be the 4343th row from the embedding matrix \mathcal{E} corresponding to the token “I” at word-index 4343. The third and sixth rows of the activation matrix will be the 1st row from the embedding matrix corresponding to the token “a” at word-index 1, and so on.

During the back propagation of training, a gradient matrix Δ of dimension $K \times D$ is generated for the embedding layer. Since, the embedding matrix \mathcal{E} is $|V| \times D$ in dimension, a reverse mapping is performed from the i^{th} row of the gradient matrix to the j^{th} row of the embedding matrix. *Since multiple rows of Δ may map on to the same row of \mathcal{E} , an updates to \mathcal{E} is an accumulation operation.*

The RNN neural network consumes \hat{E} and produces an intermediate representation of the input. The output of the last RNN layer is fed to an “output embedding” layer, which maps hidden states back to words, using inverse role of the input embedding layer. The output embedding is a fully-connected layer that projects a lower dimension data back to

the number of words in the vocabulary, so that the probability of every word can be predicted. The softmax layer following the output embedding layer, produces a normalized probability distribution over *all* words in the vocabulary. The probability of a word w at a time step t is calculated as $p(w^t|w^{<t}) = \exp(o_w^t) / \sum_{v \in V} \exp(o_v^t)$, where o_w^t is the output score from the last layer for the word w at t . The softmax normalizes the output scores into a probability distribution.

The softmax calculation is computationally most expensive because the denominator is computed over all words in the vocabulary. Typical implementations reduce the computational complexity with various techniques, the simplest (and yet effective) is sampled softmax [29], which computes the probability over a smaller, random subset over V . The sampled softmax is facilitated by making the output embedding choose a subset, e.g., 1% of the words, in the entire vocabulary; typically, the words in the input are additionally included.

Because of the sampling, during back propagation, the gradients coming from the softmax later do not match the dimensionality of the output embedding layer. Hence, the gradients are mapped back to the set of randomly chosen words during the forward pass, which is functionally similar to the back-propagation performed in the input embedding. The uniform randomness does not ensure uniqueness of the chosen set of words in the output embedding.

B. Parallelism in Language Models

We now divert our attention to parallelizing the training process. Data parallelism is the most common form of parallelism in neural networks; each processing entity (GPU in our case) holds the model but works on different K input token sequence, drawn randomly from the entire training corpus. In fact, each GPU also consumes K/c number of input sequences, where each sequence is of length c , and processes them in parallel; for brevity we refer to the entire data fed to a GPU as the *local batch size* and represent its size with the symbol K . While the forward propagation through the model can proceed unsynchronized across all GPUs, the gradient updates in each layer following the backward propagation needs to synchronize with all GPUs. The synchronization ensures that the model parameters on all GPUs are the same during the next training step. The so-called asynchronous gradient update is an active research area and out-side the scope of our work.

To update the RNN parameters, the models perform an ALLREDUCE [30] to accumulate the gradients from all GPUs. The accumulated gradients are used in updating the local weights. The communication is over large gradient matrices (e.g. LSTM layers) and hence bandwidth bound; efficient implementations use a ring all-reduce technique [31]. The input and output embedding connections are special and pose additional challenges.

During the same time step, each GPU i can have its own K training tokens: $w_{i1}, w_{i2}, \dots, w_{iK}$, different from the K training tokens on another GPU j represented by $w_{j1}, w_{j2}, \dots, w_{jK}$, which is the reason for complication in the embedding layers.

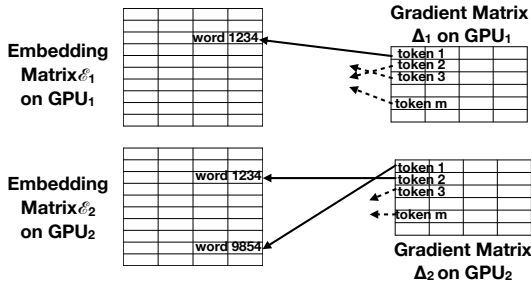


Fig. 3. GPU₁ and GPU₂ independently compute their local gradients Δ_1 and Δ_2 , respectively. However, the updates to their embedding matrices \mathcal{E}_1 and \mathcal{E}_2 needs to be synchronized. The first token (row) of Δ_1 maps to 1234th word (row) in \mathcal{E}_1 and the first token in Δ_2 maps to 9854th word in \mathcal{E}_2 . As result, one cannot accumulate gradients with an ALLREDUCE operation. LM implementations perform the space- and communication-expensive ALLGATHER to circumvent the problem.

If the p^{th} tokens is not an instantiation of the same word on the two GPUs, (that is, $w_{ip} \neq w_{jp}$), which is often the case, then the gradients computed for the p^{th} tokens (Δ_{ip} and Δ_{jp}) on two different GPUs do not map to the same row of the embedding matrix during the reverse mapping step. This is depicted in Figure 3, where the gradient for the first tokens on GPU₁ maps to the 1234th row of the embedding matrix, whereas the gradient for the first tokens on GPU₂ maps to the 9854th row of the embedding matrix. Furthermore, since the words need not be unique across the GPUs, the gradient for the second tokens on GPU₂ maps to the 1234th row of the embedding matrix. We remind that the two embedding matrices \mathcal{E}_1 and \mathcal{E}_2 must remain the same across updates.

Since gradients at the same index on two different GPUs may map to two different rows of the embedding matrix, one cannot perform an ALLREDUCE operation over all $\Delta_i = K \times D$ -dimensional dense gradients. State-of-the-art implementations, hence, perform an ALLGATHER, which collects all $K \times D$ matrices from all G GPUs ($G-1$ other GPUs to be precise) and then applies the gradients to the local embedding matrix. The ALLGATHER operation requires $\Theta(G \times K \times D)$ local memory to hold G number of Δ matrices, and the communication time is also bounded by $\Theta(G \times K \times D)$. Finally, the time to update each \mathcal{E}_i is also bounded by the $\Theta(G \times K \times D)$. Not all $G \times K$ words are unique; words can repeat within a token sequence both on the same GPU and on different GPUs. Hence, while concurrently updating different rows of \mathcal{E} using the parallelism on GPUs, *the rows under update are locked to prevent races*. Such locking is necessary even in the single GPU case since the words can repeat within a sequence presented to the same GPU.

The updates to the output embedding is analogous to the input embedding in the presence of sampled softmax due to random, sparse word selection. If each GPU computes the probability of S randomly chosen output words, during the gradient update, it has to gather the updates from all other G GPUs and then update the local output embedding matrix. The number of samples is proportional to the local batch size, that is $S \propto K$. As before, implementations perform an ALLGATHER to accomplish this task. If the output embedding

is a vector of size D , the ALLGATHER operation requires $\Theta(G \times K \times D)$ local memory to hold the entire update; the communication and local update time are bounded by $\Theta(G \times K \times D)$. Implementations may use different dimensions for input and output embeddings, but it is less common.

In summary, embedding layers are the performance limiters in LM implementations. LMs' local memory footprint grows proportional to the product of local batch size and the number of GPUs ($\Theta(G \times K)$). Since, GPUs have a limited memory ($\sim 16\text{GB}$), one cannot scale LMs beyond a handful of GPUs. LM's communication volume and GPU memory footprint grow proportional to the number of GPUs times the local batch size. Thus, large-scale language modeling (whether using a large batch size or a large number of GPUs or both) becomes communication bound, runs out of memory, and consequently fails to scale beyond a few GPUs or suffers from poor parallel efficiency; Section V provides empirical data in this regard.

III. METHODOLOGY: SCALABLE LANGUAGE MODELING

We, now, describe how we overcome the fundamental limiting factors in scaling LMs. Although, at the outset, the algorithmic complexities seem to limit scalability, studying the word distribution in a training corpus offers optimization insights. Word distribution empirically follows the well-known Zipf's power law [1]–[3]: “given some corpus of natural language utterances, the frequency of any word is inversely proportional to its rank in the frequency table. Thus, the most frequent word will occur approximately twice as often as the second most frequent word, three times as often as the third most frequent word”. We exploit this domain knowledge on the word distribution to reduce the previously shown complexity bounds on scalability. The larger the batch size or more the number of GPUs, higher the opportunity to exploit the Zipf's law frequency distribution, discussed in [4], [5].

The rest of this section describes our strategy exploiting this observation for achieving better scalability. We first explain its application to the input embedding layer. We then describe an additional optimization—controlled seeding—to make scheme applicable to the output embedding layer. We end the section with an orthogonal optimization, half-precision communication, which provides an additional improvement in scaling.

A. Exploiting word uniqueness to reduce communication and memory demands of embedding layer.

Figure 4 depicts our strategy. To give a high-level intuition, we perform an ALLGATHER over the *word indices* to know all unique words presents in a training step. Then, each GPU re-arrange its local gradients into a matrix such that a gradient vector corresponding to a given word appears at the same position (row) across all GPUs. We then perform an ALLREDUCE over the re-organized gradients.

Let the local batch of K tokens on GPU i contain $U_i \leq K$ unique words. Let the K -dimension vector \mathcal{J} on each GPU hold the word index corresponding to each token in its input sequence. Our strategy can be described in the following sequential steps.

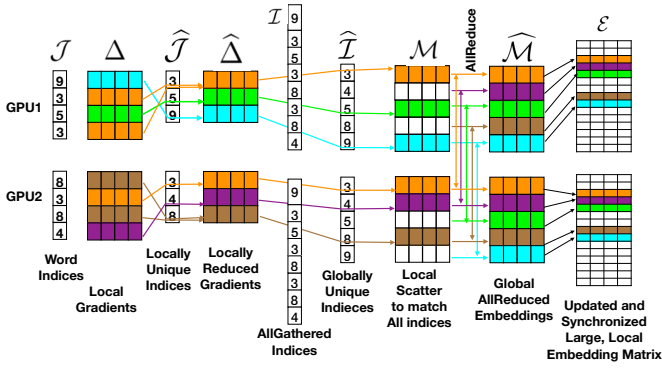


Fig. 4. A demonstration the UNIQUE approach in updating each GPU’s embedding matrix \mathcal{E} from its gradients Δ . Expensive ALLGATHER over the entire gradients is converted into a sequence of local unique index computation ($\mathcal{J} \rightarrow \hat{\mathcal{J}}$), all-gather over indices ($\hat{\mathcal{J}} \rightarrow \mathcal{I} \rightarrow \hat{\mathcal{I}}$), local scatter of gradients ($\Delta \rightarrow \mathcal{M}$) and an ALLREDUCE to produce $\hat{\mathcal{M}}$, which is used to update \mathcal{E} .

- 1) On each GPU, compute the vector $\hat{\mathcal{J}}$, which holds the word indices of only *unique* words in its input sequence. In other words, $\hat{\mathcal{J}}$ is a vector of “types” present on that GPU.
- 2) On each GPU i , perform a *local reduction* of the gradient vectors, so that the gradient vectors corresponding to the same words are accumulated into a single vector. Now, each GPU i has a gradient matrix $\hat{\Delta}_i$ of dimension $U_i \times D$.
- 3) Perform an ALLGATHER over $\hat{\mathcal{J}}$ vectors from all GPUs. This ALLGATHER consumes only $\Theta(G \times K)$ memory as opposed to the traditional ALLGATHER that required $\Theta(G \times K \times D)$ memory. Let the resulting vector be \mathcal{I} , which is same on all GPUs.
- 4) On each GPU, perform a *local filter* operation over the $G \times K$ indices (vector \mathcal{I}) to extract all unique word indices to produce vector $\hat{\mathcal{I}}$. In other words, $\hat{\mathcal{I}}$ holds all “types” in a training step. Let the elements in the $\hat{\mathcal{I}}$ be totally ordered and let us maintain a mapping from an entry in $\hat{\mathcal{J}}$ to the corresponding entry in $\hat{\mathcal{I}}$ and transitively from $\hat{\mathcal{J}}$ to $\hat{\mathcal{I}}$, which are local operations. Now, each GPU has a consistent view of all word indices present in this time step; if the p^{th} entry of $\hat{\mathcal{I}}$ on GPU i points to q^{th} row of its \mathcal{E} , so does the p^{th} entry of $\hat{\mathcal{I}}$ on another GPU j . Let each GPU infer that in total there are U_g unique words in this time step.
- 5) On each GPU i , expand the $\hat{\Delta}_i$ matrix obtained in step 2 from a $U_i \times D$ matrix into a $U_g \times D$ matrix via a local scatter operation. The non existing entries are filled with zeros. Let this expanded matrix be called \mathcal{M}_i . Note that $U_i \leq U_g \ll G \times K \ll |V|$.
- 6) Perform an ALLREDUCE over all \mathcal{M}_i , each of which is of the same $U_g \times D$ dimension. This step has communication cost of $\Theta(U_g \times D)$. Let the resulting matrix be $\hat{\mathcal{M}}$.
- 7) Update the local embedding matrix with the the values in $\hat{\mathcal{M}}$ using $\hat{\mathcal{I}}$ to map index in $\hat{\mathcal{M}}$ with row in \mathcal{E} .

The total space and communication complexities are: $\Theta((G \times K) + (U_g \times D))$, which is a significant reduction from the original $\Theta(G \times K \times D)$. Since $U_g \propto (G \times K)^\alpha$, we have

reduced both time and memory complexity from $\Theta(G \times K \times D)$ to $\Theta((G \times K)^\alpha ((G \times K)^{1-\alpha} + D))$, where α is the exponent in Zipf’s power-law in word frequency distribution.

Consider a real-word example, where the sequence length is $c = 150$, the number of sequences per GPU is 128, which makes a local batch size of $K = 150 * 120 = 19,200$, and the embedding dimension is 1792. In this setting, with 32-bit floating-point gradients, on 256 GPUs, the old scheme of ALLGATHER would require 35.2 GB of memory per GPU. However, with our *uniqueness* technique where the power-law exponent is 0.64, we would require only 0.137 GB of memory per GPU—a $256 \times$ memory saving.

An additional benefit is that since all indices are unique when updating the local model in step 7, no two indices are simultaneously attempting to update the same embedding vector in \mathcal{E} and hence no serialization bottleneck. To better appreciate this fact, imagine that in a set of updates, if 50% of the tokens are all the same highest-frequency word, the updates to their corresponding embedding vector would be serialized wasting the available parallelism on a GPU. This problem is eliminated in our update scheme that has no duplicate words.

B. Controlled randomness to reduce communication and memory demands of softmax layer.

The *uniqueness* technique is not directly applicable when updating the *output* embedding matrix in the presence of sampled softmax because the sampling can choose different words on different GPUs. For a large vocabulary, the probability of choosing the same word at the same index is minuscule; and the total words selected by all the GPUs grows proportional to the number of GPUs times the local batch size. Thus, we lose the power-law distribution of words when updating the output embedding with the gradients.

An easy approach would be to force all GPUs to use the same random seed, so that they all choose the same set of random words in each time step. Although, the same seed makes the updates to the output embedding amenable to the same optimization described in Section III-A, the loss of randomness leads to loss of diversity, which results in poor learning and degrades accuracy. Thus, there is a trade-off: each GPU with a different random seed has a good accuracy but poor scalability, whereas each GPU with the same random seed has a poor accuracy but good scalability.

Interestingly, the trade-off is not binary; there is a spectrum of choices to make. Instead of all same seed or all different seeds, we make a subset of GPUs use the same seed. We evaluated the number of seeds equal to \log_2 , \log_e , and \log_{10} of the number of GPUs. *We empirically observed that the number of different seeds needed to produce accuracy matching all different seeds matches the power law.* Meaning, with G GPUs, we only need G^α unique random seeds to achieve a very good accuracy (empirically $\alpha = 0.64$) while enjoying the benefits of few unique words and hence less communication and memory overhead. We present the details in Figure 7 in Section V.

Equipped with this technique, the rest of the procedure in updating the output embedding matrix is the same as that of

the input embedding layer. When S is the number of sampled words per GPU, the total space and communication complexity of the updates performed in the output embedding layer are: $\Theta((G \times S) + (U_g \times D))$, which is a significant reduction from the original $\Theta(G \times S \times D)$. Since $U_g \propto (G \times S)^{0.64}$, in practice, we have reduced both time and memory complexity from $\Theta(G \times S \times D)$ to $\Theta((G \times S)^{0.64} \times D)$.

C. Lower precision to reduce communication

Deep learning models are usually trained using 32-bit floating point (FP32) numbers. However, due to the increased gap between computation required vs. delivered [32] for deep learning applications, reduced precision (e.g. 16-bit floating point numbers, FP16) is gaining popularity. Recently, [33], [34] showcased that FP16 based models can be trained with negligible loss of accuracy. It uses a *loss-scaling* technique, to minimize the number of gradient values becoming zeros, due to lower precision. The idea is to multiply the training loss (e.g. cross-entropy) by a scaling factor, F (e.g. 256, 512, and 1024) before computing gradients and then divide the gradients by F before updating the weights. This method reduces the memory footprint by 50% and works well on a wide range of applications including image recognition and machine translation [33].

We use the same concept of lower precision to reduce communication among the GPUs. We down-cast each FP32 tensor to FP16, communicate, and up-cast the FP16 tensor to FP32 at the receiving end. This reduces the communication by 50%. To minimize loss introduced by lower precision, we perform *compression-scaling*, that is, multiply the FP32 tensor by a scaling factor, F before down-casting, and divide again by F after up-casting. We call this method *compression*.

IV. EXPERIMENTAL SETUP

We performed all the experiments on a 50-node cluster. The software and hardware configurations are tabulated below.

TABLE II
SYSTEM CONFIGURATION.

# Nodes	50
Interconnect	Infiniband FDR @ 15GB/s bidirectional bandwidth
CPUs/node	2 × 20-core Intel Xeon E5-2660 v3 @2.6 GHz
Memory/node	400GB DDR
GPUs/node	8 × GeForce GTX Titan X @ 32 GB/s PCIe bidirectional b/w
GPU memory	12GB HBM2
peak FLOP/GPU	6.1 TFLOP/s (32-bit floating point numbers)
Software	Tensorflow 1.4 [35], CUDA 8.0.61, CUDNN 6.0.20, cuda-aware OpenMPI 2.0.1

We use one GPU per MPI process in all of our experiments. Communication among the GPUs (both inter and intra-nodes) use cuda-aware MPI collectives incorporated in Tensorflow.

A. Datasets

We used four datasets in our experiments, three in English and one in Chinese. One of them, the 1-Billion word [6], is the commonly used one to perform language modeling experiments [36]. We used the Gutenberg [7] dataset to better understand that our techniques are dataset independent. We used the Amazon Reviews dataset [9], which was used in

a recent scaling paper, [21]. We finally used a subset of an internal Chinese dataset curated from Baidu’s internet forum called *Tieba* [10] to perform a Hero scale run using 192 GPUs. To train the models and to test the accuracy, we split the the first two datasets into 99:1 ratio and the last two into 1000:1 ratio (similar to [21]). Each split is created by sampling without replacement and a fixed random seed. The vocabulary for character language model includes all alphanumeric characters and common symbols (98 in English and ~15K in Chinese). For word language models, we use the 100,000 most frequent words after lower-casing and tokenization [37] as the vocabulary for each corpus. The number of unique words can range from 2M to 24M in the corpora we considered, but vocabularies created by this simple procedure account for 99% of the text in each data set. A summary of all the above datasets is presented in Table I.

B. Model Architectures

To analyze scaling and accuracy, we take the character and word language models as test-cases for small and large vocabulary, respectively. For word language model, we use the baseline LSTM based SOTA model from [36]. The model consists of one LSTM layer with 2048 cells. The projection dimension we used is 512. The batch size per GPU is 32 and sequence length is 20. This configuration with ~800K vocabulary (as used in [36]) requires more than 9.8 GB of memory for the model parameters and activations. We therefore used a reduced vocabulary size of ~ 100K so that required memory is much lower (1.3 GB) and also the CPU-GPU traffic reduces significantly. In the experiments, we used stochastic gradient descent (SGD) for optimizing per-sequence word cross-entropy loss using a sampled softmax layer, with 1024 random samples per GPU. The learning rate is $0.2 \times \log_e(|nodes|)$ with decay factor ranging from 0.85 to 0.95 in the experiments. In our experiments, each *node* consists of 8 GPUs.

For the character language model, we use the SOTA model similar to [38]. The model consists of a recurrent highway network (RHN) layer of depth 10, each with 1792 LSTM cells. The model consists of 213 million parameters. We use 128 batch size per GPU with sequence length of 150. We use *Adam* with weight decay and dropout for optimizing the character cross-entropy loss using a full softmax layer. We used a learning rate of $10^{-3} \times \log_e(|nodes|)$ with decay factor ranging from 0.85 to 0.95 in the experiments.

V. RESULTS AND ANALYSIS

In this section, we present the experimental results obtained by our proposed methodology. We use word and character language model as test-cases for large and small vocabulary, respectively. We showcase accuracy and speedup comparison along with details analysis for 1-Billion and Gutenberg datasets using 16, 32 and 64 GPUs. We later present results of a *hero-scale* run on the *Tieba* dataset using 192 GPUs. Finally, we compare our results with existing works on the Amazon review dataset.

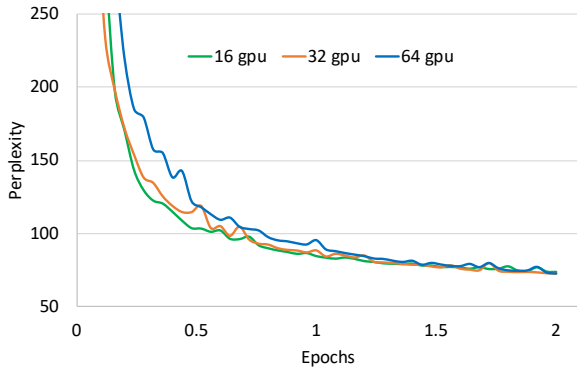


Fig. 5. Accuracy of word language model on the 1-Billion word dataset using 16, 32, and 64 GPUs.

TABLE III

PER EPOCH TIME (HOURS) ON TITAN X GPUS FOR WORD LM USING 1-BILLION WORD DATASET. 8-GPUS IS THE BASELINE FOR COMPUTING PARALLEL EFFICIENCY. * => OUT OF GPU MEMORY.

GPUs	Without Our Technique		With Our Technique	
	Time (hours)	Parallel Efficiency	Time (hours)	Parallel Efficiency
8	35.1	100%	14.6	100%
16	41.1	43%	8.1	90%
24	40.4	29%	6.4	76%
32	*	-	5.4	67%
64	*	-	4.5	40%

A. Word Language Model

We first present the accuracy and speedup achieved by the word language model with large vocabulary ($\sim 100K$). We use three combinations of GPUs, 16, 32, and 64, to perform the scaling experiments with batch size of 512, 1024, and 2048, respectively. The sequence length used was 20, therefore, per iteration the number of tokens (words) processed was 10240, 20480, and 40960, respectively for the three GPU combinations. We use perplexity (lower is better) to compare accuracy, which measures how well a model is capable to compute the probability distribution to predict words or characters.

Figure 5 shows the accuracy validation perplexity up to 2 epochs for the 1-Billion dataset. The perplexity becomes indistinguishable with increasing epochs. For example, at Epoch 1, the perplexities are 84.3, 87.9, and 95.3 for 16, 32, and 64 GPUs. The values reduces to 73.5, 72.1, and 72.4, respectively at Epoch 2. We realized that 32 and 64 GPUs produce better perplexity compared to 16 GPUs run. The trend continues in the later epochs as well (e.g. 67.7, 63.7, and 63.6 at epoch 5). We achieved similar trend with accuracy for the Gutenberg dataset. For example, we found perplexity of 76.7, 77.4 and 81.1 at epoch 1 whereas these values become 63.0, 63.6, and 67.1 at epoch 3 using 16, 32, and 64 GPUs respectively. We use 0.2 as the base learning rate (for 8 GPUs) and then used a multiplying factor of $\log_e |nodes|$ (e.g. 0.41 for 64 GPUs) as we increase the number of GPUs.

Table III shows the time taken per epoch by the word language model for 1-Billion word dataset while varying the number of GPUs, keeping the local batch size fixed. Using our techniques, we found that per epoch time using 8 GPUs is

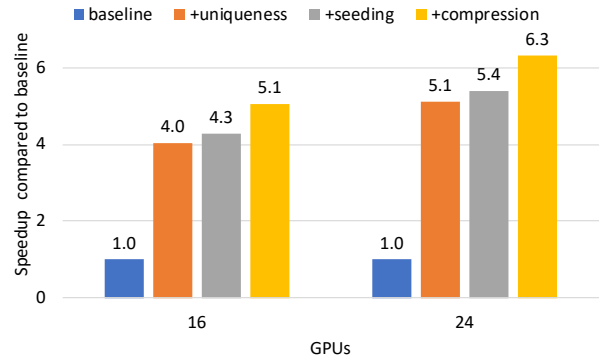


Fig. 6. Speedup achieved using our techniques, uniqueness, seeding, and compression (lower precision) compared to the baseline (without these techniques) word language model on 16 and 24 TitanXx8 GPUs.

14.6 hours. If we increase the number of GPUs by $8\times$ (i.e. 64 GPUs), the training time reduces to 4.5 hours ($3.2\times$ speedup). Compared to the 8 GPUs run without our techniques, the speedup becomes $7.7\times$. Without our techniques the code struggles to achieve parallel efficiency of 29% using 24 GPUs and goes out of memory with more GPUs. In contrast, our techniques deliver 76% parallel efficiency using 24 GPUs. The value become 40% when we use 64 GPUs using our approaches (> 24 GPUs run without our techniques). We found similar results for the Gutenberg dataset ($2.4\times$ speedup using $8\times$ more GPUs and a parallel efficiency of 30% on 64 GPUs). Compared to the 8 GPUs run without our techniques, the speedup becomes $6.3\times$. The lower speedup in word LM when compared to our own 8 GPUs run is due to the low computational intensity (136 GFLOP/iter) of word LMs; character LMs achieve higher speedup (2,721 GFLOP/iter) as shown in the next section. We obtained 2.44 TFLOP/sec (40% of peak FLOPS) in the experiments.

Figure 6 shows the performance improvement up by each of the three techniques—*uniqueness*, *seeding*, and *compression*. To do this, we present the results obtained from using 16 and 24 GPUs on 1-Billion word dataset. We consider the baseline that does not use our techniques [38]. *Uniqueness* delivers a $4\times$ performance improvement (speedup). The speedup closely matches to the ratio of total and unique words (Figure 1), which is $3.4\times$ at 16 GPUs. The *seeding* and *compression* techniques give additional 7% and 18% performance improvements, respectively, thus reaching a total of $5.1\times$ speedup compared to the baseline. The speedup was found to be higher (e.g. $6.3\times$ on 24 GPUs as shown in the Figure 6) as the gap of unique words vs. total words increases with the number of GPUs. The peak GPU memory in use (not shown), without our techniques, grows linearly: 3.9 GB, 7.1 GB, and 10.3 GB per GPU at 8, 16, and 24 GPUs, respectively and goes out of memory after that. In contrast, the peak GPU memory in use, with our techniques, remains almost steady—1.19 GB at 8 GPUs, 1.20 GB at 24 GPUs, and 1.21 GB at 64 GPUs. Thus, we achieve $8.6\times$ memory reduction when using 24 GPUs.

We now divert attention how our techniques may influence accuracy. The *uniqueness* technique only changes the flow of

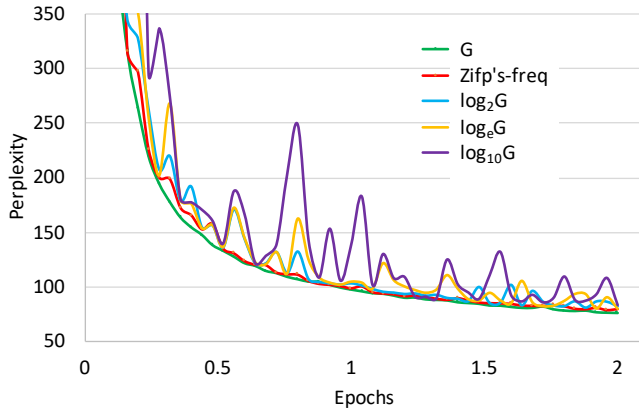


Fig. 7. Different seeding techniques used in the sampled softmax layer for word language model using 64 GPUs.

computation as discussed in Section III-A, and hence produces the same accuracy as the baseline for word language model.

Figure 7 shows the impact of different seeding techniques on accuracy, which is used in the output embedding layer to compute sampled softmax for word language model. We used a different seed on each GPU (line with label G) and also the number of seeds equal to \log_2 , \log_e , and \log_{10} of the number of GPUs. We have also performed experiments where the number of seeds follows the word frequency distribution (line with label *Zipf's-freq*). Decreasing the number of seeds makes the accuracy of the training curve less stable (e.g. \log_2 shows more close perplexity as G than \log_{10}). Seeding with *Zipf's-freq* produces similar perplexities as G seeds and offers a pareto optimal setting.

The *compression* technique loses lower precision bits, hence accuracy is expected to be lower. But *compression-scaling* (Section III-C) regains the same accuracy. For example, the perplexity of word language model after 1 epoch on 16 GPUs with and without compression are 84.12 and 84.68, respectively.

B. Character Language Model

Figure 8 shows the accuracy (perplexity) up to 2 epochs for character language model with small vocabulary (~ 100) on the 1-Billion dataset. Similar to the word language model, we use 16, 32, and 64 GPUs, to perform the scaling experiments with a batch size of 2048, 4096, and 8192 (hence 0.3M, 0.6M and 1.2M total characters), respectively. As the figure shows, our three sets of experiments produces similar perplexities. We observe that gap of perplexities reduces as we progress towards further epochs. For example, perplexity difference between 16 and 32 GPUs at epoch 1 is 4%, whereas at epoch 2 and 4, the gap becomes 2% and 0.01%, respectively. We observe similar results when comparing 16 GPUs with 64 GPUs (the gap is 5% at epoch 1 and 1% at epoch 5). Although the perplexity with higher GPUs has higher perplexity at any point in the figure, running a few additional iterations produces the same accuracy as the lower number of GPUs (e.g. perplexity of 2.27 using 16 and 32 GPUs at epoch 3 and 3.4, respectively).

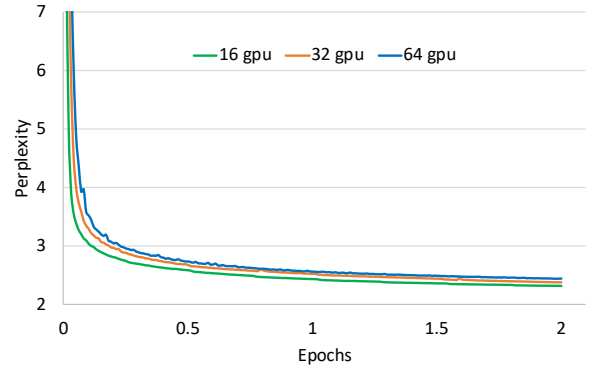


Fig. 8. Accuracy of character language model on the 1-Billion word dataset using 16, 32, and 64 GPUs.

We observe similar results on the Gutenberg dataset. At epoch 1, the perplexity of 16 and 32 GPUs are 2.78 and 2.85, respectively. However, at epoch 3, the corresponding values become 2.53 and 2.54. Similar results have been observed when comparing the accuracy of 16 vs. 64 GPUs. Note that we increased the base learning rate (10^{-3} for 8 GPUs) by a multiplying factor of $\log_e |nodes|$ (e.g. 2.07×10^{-3} for 64 GPUs), similar to the word LM.

We now discuss how the training time per epoch for the 1-Billion word dataset reduces as we increase the number of GPUs, while keeping the local batch size fixed. Table IV shows the taken time and parallel efficiency with and without our techniques. We use the runtime using 8 GPUs as the baseline for comparison among the experiments. Our techniques take 23.2 hours per epoch using 8 GPUs and increasing the GPUs to 64, the time reduces to 3.5 hours. We achieve $6.6\times$ speedup (with 82% parallel efficiency) using $8\times$ more GPUs. At 24 GPUs, while our technique delivers 94% parallel efficiency, without our techniques, the baseline delivers 81% parallel efficiency. Beyond 24 GPUs, the baseline goes out of memory, whereas our implementation continues to scale—a demonstration of the usefulness of our *uniqueness* and *compression* techniques detailed in Section II. Note that *seeding* technique was not used for character LM as the vocabulary size is small, hence full softmax was used instead of sampled softmax layer. We achieved similar speedup ($6.7\times$ using $8\times$ GPUs compared to 8 GPUs baseline) when we experiment on the Gutenberg dataset. We obtained 3.95 TFLOP/sec (64% of peak FLOPS) in the character LM experiments. We mention in passing that the number of unique *characters* becomes constant (reaching the size of the small vocabulary) as we keep increasing the batch size (thus GPUs) in character language model.

Table IV shows an improvement in performance when compared to the same number of GPUs without our techniques. For example, on 16 GPUs, we found *uniqueness* contributes to 23% runtime reduction. We observe limited gain (e.g. 2% on 16 GPUs) using the *compression* technique for character LM. This is mainly due to the fact that the character language model has higher number of tensors (> 20), each needs to down-cast (FP32 \rightarrow FP16) and up-cast (FP16 \rightarrow FP32), thus adds an overhead to get benefit of the compression technique.

TABLE IV
PER EPOCH TIME (HOURS) ON TITAN X GPUS FOR CHARACTER LM
USING 1-BILLION WORD DATASET. 8-GPU IS THE BASELINE TO COMPUTE
PARALLEL EFFICIENCY. * => OUT OF GPU MEMORY.

GPUs	Without Our Technique		With Our Technique	
	Time	Parallel Efficiency	Time	Parallel Efficiency
8	25.7	100%	23.2	100%
16	14.5	89%	12.9	96%
24	10.6	81%	8.2	94%
32	*	-	6.8	86%
64	*	-	3.5	82%

When we compared the accuracy, we found our *compression-scaling* (Section III-C) technique regains the same accuracy as without using compression. For example, the perplexity of character language model after 1 epoch on 64 GPUs with and without compression are 2.58 and 2.59, respectively.

C. Hero Scale Run (Tieba dataset, 192 GPUs)

In this section, we apply our techniques to train massive data that was impractical previously. We improve the accuracy of language modeling on the Tieba [10] dataset, keeping the training time in a reasonable range while scaling to more GPUs and hence training on more data.

We take two subsets, 1 and 4 Billion Chinese characters from the Tieba dataset [10] (32 Billion). We use the same validation set to test accuracy of all three datasets. The vocabulary we used consists of 15,437 characters ($\sim 150\times$ larger than English, thus a demonstration of scaling character language model with large vocabulary). We perform weak scaling using 6, 24, and 192 GPUs for the 1B, 4B, and 32B datasets respectively. The corresponding learning rate is 2×10^{-4} , 4×10^{-4} , and 5×10^{-4} . Table V shows that increasing the data size from 1B by $4\times$ and $32\times$, the training taken time per epoch increases by only $1.04\times$ and $1.25\times$, respectively. We achieve a total of 0.76 PFLOP/s using 192 GPUs. Compared to 6 GPUs with 3GB corpus, a 12 GB corpus on 24 GPUs delivers a 20% accuracy improvement and a 93 GB corpus on 192 GPUs delivers 35% accuracy improvement.

Since the internal Tieba dataset does not have public baselines on accuracy, we compute the compression ratio as a metric to demonstrate the competitiveness of our results on this corpus. We chose this metric as perplexity is an indication of performance in text compression. We compute the compression ratio by dividing the corpus size by the product of bits per character and total number of characters in the corpus. [21] showed a bit per character (i.e. $\log_2(\text{perplexity})$) of 1.11 for the Amazon review dataset with comparable batch size, which equates to a compression ratio of 6.8. For the Tieba dataset (93GB, 34 Billion Characters), we achieve a comparable compression ratio (e.g. the perplexity of 11.1 equates to compression ratio of 6.3).

D. Comparison with the Existing Results

We compare our results with a recent work on scaling language modeling [21], despite the fact that our implementation is capable of scaling on more GPUs and larger vocabularies (i.e. 192 GPUs, 15K and 100K vocabulary for

TABLE V
TIEBA RESULTS.

Characters (Billion)	Corpus (GB)	GPUs	Batch Size	Time (hours)	Perplexity (1 epoch)
1.07	3	6	768	27	17.06
4.29	12	24	3,072	28	13.6
34.36	93	192	12,288	34	11.1

character and word LM, respectively) than [21] (128 GPUs and small vocabulary of 100). Although the dataset they used in the experiments is publicly available (e.g. Amazon review [9]), the infrastructure is the most recent one (October, 2018) and specialized. For example, the 128 GPUs used were V100 (peak 125 TFLOP/s, 16GB of HBM2 memory, and NVLink to communicate among GPUs). Since we do not have access to such infrastructure, we perform experiments using 64 Titan X GPUs (peak 6.1 TFLOP/s, 12GB of HBM2 memory, and PCIe for communication). Using the above discussed RHN based character LM, we achieve an accuracy of 1.208 BPC (bit per character) compared to 1.218 reported in [21] after 1 epoch. When compared the training time, we take 17.6 hours, $14\times$ longer than [21], but using $41\times$ less powerful infrastructure (16 PFLOP/s vs. 0.39 PFLOP/s), leading to a rough gain of $2.9\times$. The gain increases to $3.3\times$ as we train to 3 epochs with an accuracy of 1.11 BPC.

VI. RELATED WORK

Compute required to train deep neural networks jumped $15\times$ and compute delivered by GPUs increased by $10\times$, just in 2 years, 2015-2017 [32]. Large-scale training has been of significant interest to reduce the training time. Most of the recent scaling efforts are centered around vision applications, such as image recognition and segmentation. For example, [24] trains ResNet-50 model using ImageNet dataset (1.2 million images) [39] in an hour using 256 Tesla P100 GPUs. [24] reduces the training time to 20 minutes using 2048 Intel Xeon Phi coprocessors. [22] goes further reducing the training time to 15 minutes using 1024 Tesla P100 GPUs.

The importance of scaling has also been realized in the neural language processing (NLP) domain, specially in language modeling, which plays a key role in traditional NLP tasks [36]. For example, [36] performs experiments on a wide range of RNN based models and proposed a CNN based softmax loss computation, which improves accuracy on 1-Billion word dataset. The paper uses 32 Tesla K40 GPUs with asynchronous gradient updates. However, it has been shown that synchronous SGD can often converge to a better final accuracy than asynchronous SGD [40]. Moreover, asynchrony could effectively increase the momentum which is part of why it tends to diverge so easily [41], [42]. [25] explores an online distillation-based large-scale distributed training method. The paper shows that codistillation works well on a wide range of applications including language modeling using 128 GPUs. But in the distillation approach, multiple models are trained in parallel, which significantly increases computation. [26] scales both on word and character language model using eight NVIDIA Volta GPUs. The dataset for character LM were

$\sim 90M$ and for word LM, it was $\sim 100M$. [21] scales character LM (small vocabulary of 100) using up to 128 NVIDIA Volta GPU using mixed precision training on 40 GB of Amazon review dataset.

VII. CONCLUSIONS

Language modeling is a central problem in natural language processing, which is used in many applications such as speech recognition and machine translation. Prior work on language modeling has achieved limited scalability. The ALLGATHER operations performed in the input and output *embedding* layers of language models require large memory footprint which quickly grows out of GPU memory limits and demand large volume data exchange among GPUs. In this paper, we showed how Zipf’s law can be used to reduce the asymptotic complexity of both memory (within a GPU) and communication (across GPUs) and hence scale up language modeling to take advantage of more training data and more GPUs. Using several datasets, we demonstrate $6.7\times$ (character LM) and $6.3\times$ (word LM) speedup by scaling to $8\times$ more GPUs with negligible loss of accuracy. Finally, we weak scale LM from six to 192 GPUs, which allows us to scale training from 3GB to 93GB of the Chinese Tieba dataset while taking only $1.25\times$ more training time. This weak scaling delivers 35% more accuracy in predictions.

REFERENCES

- [1] G. K. Zipf, *Human Behaviour and the Principle of Least Effort: an Introduction to Human Ecology*. Addison-Wesley, 1949.
- [2] Wikipedia, “Zipf’s law,” https://en.wikipedia.org/wiki/Zipf%27s_law, (Accessed on 10/12/2018).
- [3] G. K. Zipf, “The Psycho-Biology of Language,” *Linguistic Society of America*, vol. 12, no. 3, pp. 196–210, 1936.
- [4] S. Yu, C. Xu, and H. Liu, “Zipf’s law in 50 languages: its structural pattern, linguistic interpretation, and cognitive motivation,” *arXiv:1807.01855*, 2018.
- [5] M.-S. Isabel, F.-C. Francesc, and C. Alvaro, “Large-Scale Analysis of Zipf’s Law in English Texts,” *PLOS ONE*, 2016.
- [6] C. Chelba, T. Mikolov, M. Schuster, Q. Ge, T. Brants, P. Koehn, and T. Robinson, “One billion word benchmark for measuring progress in statistical language modeling,” *arXiv preprint arXiv:1312.3005*, 2013.
- [7] P. di Miceli, “Project Gutenberg,” <https://www.gutenberg.org/>, 2018.
- [8] C. Buck, K. Heafield, and B. van Ooyen, “N-gram Counts and Language Models from the Common Crawl,” in *Proceedings of the Language Resources and Evaluation Conference*, Reykjavik, Iceland, May 2014. [Online]. Available: <http://commoncrawl.org/>
- [9] J. McAuley, C. Targett, Q. Shi, and A. van den Hengel, “Image-Based Recommendations on Styles and Substitutes,” ser. SIGIR ’15. New York, NY, USA: ACM, 2015, pp. 43–52.
- [10] BAIDU, “Baidu Tieba Log File,” <https://tieba.baidu.com/index.html>, 2018.
- [11] K. W. Church and R. L. Mercer, “Introduction to the Special Issue on Computational Linguistics Using Large Corpora,” *Computational Linguistics*, vol. 19, no. 1, pp. 1–24, Mar. 1993. [Online]. Available: <http://dl.acm.org/citation.cfm?id=972450.972452>
- [12] C. Shannon, “The mathematical theory of communication,” *Bell System Technical Journal*, vol. 27, pp. 398–403.
- [13] S. Claude, “Prediction and entropy of printed English,” *Bell System Technical Journal*, vol. 30, pp. 50–64.
- [14] S. Merity, B. McCann, and R. Socher, “Revisiting Activation Regularization for Language RNNs,” *CoRR*, vol. abs/1708.01009, 2017.
- [15] M. Luong, H. Pham, and C. D. Manning, “Effective Approaches to Attention-based Neural Machine Translation,” *CoRR*, vol. abs/1508.04025, 2015. [Online]. Available: <http://arxiv.org/abs/1508.04025>
- [16] D. Amodei et al., “Deep Speech 2: End-to-End Speech Recognition in English and Mandarin,” *CoRR*, vol. abs/1512.02595, 2015.
- [17] A. M. Rush, S. Chopra, and J. Weston, “A Neural Attention Model for Abstractive Sentence Summarization,” *CoRR*, vol. abs/1509.00685, 2015.
- [18] M. E. Peters, M. Neumann, M. Iyyer, M. Gardner, C. Clark, K. Lee, and L. Zettlemoyer, “Deep contextualized word representations,” in *Proc. of NAACL*, 2018.
- [19] A. Radford, K. Narasimhan, T. Salimans, and I. Sutskever, “Improving language understanding by generative pre-training,” <https://blog.openai.com/language-unsupervised/>, 2018, accessed: 2018/10/15.
- [20] M. Banko and E. Brill, “Scaling to very very large corpora for natural language disambiguation,” in *39th annual meeting on association for computational linguistics*, 2001, pp. 26–33.
- [21] R. Puri, R. Kirby, N. Yakovenko, and B. Catanzaro, “Large Scale Language Modeling: Converging on 40GB of Text in Four Hours,” *ArXiv e-prints*, Aug. 2018.
- [22] T. Akiba, S. Suzuki, and K. Fukuda, “Extremely Large Minibatch SGD: Training ResNet-50 on ImageNet in 15 Minutes,” *CoRR*, vol. abs/1711.04325, 2017.
- [23] Y. You, Z. Zhang, C. Hsieh, and J. Demmel, “100-epoch ImageNet Training with AlexNet in 24 Minutes,” *CoRR*, vol. abs/1709.05011, 2017.
- [24] P. Goyal, P. Dollár, R. B. Girshick, P. Noordhuis, L. Wesolowski, A. Kyrola, A. Tulloch, Y. Jia, and K. He, “Accurate, Large Minibatch SGD: Training ImageNet in 1 Hour,” *CoRR*, vol. abs/1706.02677, 2017.
- [25] R. Anil, G. Pereyra, A. Passos, R. Ormándi, G. E. Dahl, and G. E. Hinton, “Large scale distributed neural network training through online distillation,” *CoRR*, vol. abs/1804.03235, 2018.
- [26] S. Merity, N. S. Keskar, and R. Socher, “An Analysis of Neural Language Modeling at Multiple Scales,” *CoRR*, vol. abs/1803.08240, 2018.
- [27] M. Stephen, S. K. Nitish, and S. Richard, “Regularizing and Optimizing LSTM Language Models,” *CoRR*, vol. abs/1708.02182, 2017.
- [28] Y. Bengio, R. Ducharme, P. Vincent, and C. Jauvin, “A neural probabilistic language model,” *Journal of machine learning research*, vol. 3, no. Feb, pp. 1137–1155, 2003.
- [29] W. Chen, D. Grangier, and M. Auli, “Strategies for training large vocabulary neural language models,” *arXiv:1512.04906*, 2015.
- [30] Y. Ueno and K. Fukuda, “Technologies behind Distributed Deep Learning: AllReduce,” <https://preferredresearch.jp/2018/07/10/technologies-behind-distributed-deep-learning-allreduce/>, 2018.
- [31] A. Gibiansky, “Bringing HPC techniques to deep learning,” <http://research.baidu.com/bringing-hpc-techniques-deep-learning>, 2017.
- [32] R. Kim, “Flashblade Now 5X Bigger, 5X Faster,” <https://blog.purestorage.com/flashblade-now-5x-bigger-5x-faster>, 2017.
- [33] P. Micikevicius, S. Narang, J. Alben, G. Diamos, E. Elsen, D. Garcia, B. Ginsburg, M. Houston, O. Kuchaev, G. Venkatesh et al., “Mixed precision training,” *arXiv preprint arXiv:1710.03740*, 2017.
- [34] M. Patwary, S. Narang, E. Undersander, J. Hestness, and G. Diamos, “Experimental Evaluation of Mixed Precision Training for End to End Applications,” <http://research.baidu.com/Blog/index-view?id=103>.
- [35] M. Abadi et al., “TensorFlow: Large-scale machine learning on heterogeneous systems,” 2015, software available from tensorflow.org. [Online]. Available: <https://www.tensorflow.org/>
- [36] R. Józefowicz, O. Vinyals, M. Schuster, N. Shazeer, and Y. Wu, “Exploring the Limits of Language Modeling,” vol. abs/1602.02410, 2016.
- [37] S. Bird, E. Klein, and E. Loper, *Natural Language Processing with Python*, 1st ed. O’Reilly Media, Inc., 2009.
- [38] J. Hestness, S. Narang, N. Ardalani, G. F. Diamos, H. Jun, H. Kianinejad, M. M. A. Patwary, Y. Yang, and Y. Zhou, “Deep Learning Scaling is Predictable, Empirically,” *CoRR*, vol. abs/1712.00409, 2017.
- [39] J. Deng, W. Dong, R. Socher, L.-J. Li, K. Li, and L. Fei-Fei, “ImageNet: A Large-Scale Hierarchical Image Database,” in *CVPR09*, 2009.
- [40] J. Chen, X. Pan, R. Monga, S. Bengio, and R. Jozefowicz, “Revisiting distributed synchronous SGD,” *arXiv preprint arXiv:1604.00981*, 2016.
- [41] I. Mitliagkas, C. Zhang, S. Hadjis, and C. Ré, “Asynchrony begets momentum, with an application to deep learning,” in *Communication, Control, and Computing (Allerton)*. IEEE, 2016, pp. 997–1004.
- [42] P. H. Jin, Q. Yuan, F. Iandola, and K. Keutzer, “How to scale distributed deep learning?” *arXiv preprint arXiv:1611.04581*, 2016.